

Evaluation of Electrospinning Process Parameters of Poly Lactic-Co-Glycolic Acid and Hydroxyapatite Nanocomposite Nanofibrous Scaffolds

Amir Doustgani, Ebrahim Ahmadi

Chemical Engineering Department, University of Zanjan, Zanjan, IRAN

Correspondence to:

Amir Doustgani email: doustgani@znu.ac.ir

ABSTRACT

Electrospinning recognized as a simple and inexpensive process for producing continuous polymeric nanofibers with diameters ranging from several micrometers down to tens of nanometers. In this study, an electrospun nanofibrous scaffolds based on lactic-co-glycolic acid (PLGA) and nanohydroxyapatite (nano-HA) was developed. The fiber morphology and mean fiber diameter of prepared nanofibers were investigated by scanning electron microscopy. FTIR analysis demonstrated that there were strong intramolecular interactions between the molecules of PLGA and nano-HA. A more systematic understanding of process parameters was obtained and a quantitative relationship between electrospinning parameters and average fiber diameter was established by using response surface methodology. A response surface function was empirically determined by central composite design using fiber diameter as an observed response and the electrospinning parameters such as concentration, distance, applied voltage, temperature and flow rate as variables. The regression coefficient of the model was found to be 0.938. The predicted fiber diameter was in good agreement with the experimental result. PLGA/nano-HA nanofibrous scaffolds could be good candidates for tissue engineering applications.

Keywords: Electrospinning, Nanofibers, Optimization, Response surface method

INTRODUCTION

Electrospinning is a relatively cost-effective technique for producing nanofibers from a variety of polymeric materials with fiber diameters ranging from 50 to 500 nm dimensional scales. The technique is very promising and versatile since it facilitates the production of multifunctional nanofibers from a variety of polymers, polymer blends, composites and ceramics [1,2]. The basis of electrospinning is application of a strong electric field. This applied electric field results in an unstable jet formation with

fibers continuously collected on the substrate plate. The stretching action of the jet combined with the evaporation of the solvent material allows for the fibers to be stretched into the nanometer scale [3,4]. Polymer nanofibers have potential applications as membrane filters, scaffolds for tissue engineering, wound dressing and drug delivery [5-14]. Several parameters like the applied voltage, polymer flow rate, solution concentration, molecular weight of the polymer, operating temperature, relative humidity, collector type, diameter of the needle and tip to collector distance affects the electrospinning jetting process [15,16]. It was previously shown, for instance, that the strength of the nanofibrous mats produced by electrospinning is sensitive to fiber diameter [17]. Therefore, it is important to have control over the fiber diameter which is a function of material and process parameters. Despite the relatively early introduction of the electrospinning process, the effect of the process and material parameters on the fiber formation of the thin mat is still under investigation. It should be noted that the observations on individual effects of process and material variables by one-factor-at-a-time approach may be misleading. The Response surface methodology (RSM) is a combination of mathematical and statistical techniques useful for modeling and optimizing the effects of several independent variables on the response. This approach enables us to explore single factor and the interdependency of multiple factors simultaneously. The developed mathematical model incorporates a design of experiments (DOE) approach and regression analysis while incorporating the statistical significance of the chosen parameters. RSM has been used successfully for material and process optimization in numerous studies [18-19]. Sukigara et al. [20] employed RSM to model mean fiber diameter of electrospun regenerated Bombyx mori silk with electric field and concentration at two spinning distances. Increasing the concentration at

constant electric field resulted in an increase in mean fiber diameter. Different impacts for the electric field were observed depending on solution concentration. Gu et al. [19], also exploited the RSM for quantitative study of polyacrylonitrile (PAN). They reported no significant effect of voltage on the processing of PAN nanofibers. Thus, an overview of the processing variables and their effect on responses could be obtained using RSM. In this study, a systematic statistical approach has been adopted to obtain optimum diameter of the electrospun nanofibers with different process conditions. The influence of process conditions on the diameter of the electrospun nanofibers was carried out using central composite design. RSM was used to develop a mathematical equation between the process parameters on average nanofiber diameter.

EXPERIMENTAL

Materials

PLGA (85:15) with an average molecular weight of 66–107 kD was purchased from Sigma-Aldrich. HA nanopowder with less than 200 nm particle size was obtained from Sigma-Aldrich. Chloroform was purchased from Merck (Germany). All reagents and chemicals in this study were used without further purification.

Solution Preparation and Electrospinning

Initially Nano-HA at five different contents (0, 7.5, 15.0, 22.5, 30.0 w/w %) was added in chloroform and sonicated at room temperature for 30 min to disrupt possible agglomerates. Then, 1.2 g of PLGA pellets were added to 10 ml of the nano-HA/Chloroform dispersion. This was followed by magnetic stirring until the polymer dissolved completely. nano-HA/PLGA nanofibrous scaffolds were produced by an electrospinning machine (ANSTCO-RN/I, Asian Nanostructures Technology Co., Iran). Prepared solutions with different amounts of nano-HA, were fed into plastic syringes and then placed on a syringe pump used to dispense the solution at a controlled rate and a high voltage electric field (Nano spinner TM, Iran) was applied to draw the ultra-fine fibers from the spinneret. The collector was a rotating cylindrical drum which was placed at different distances from the needle. The electrospun nanofibers were subsequently vacuum dried so that any residual solvent present in the fibers could be removed.

Characterization of Nanofibers Morphology

The surface morphology of the electrospun fibers was characterized by scanning electron microscopy (SEM; Vega II XMU instrument Tescan, Czech Republic). Average fiber diameter of nanofibrous mats were calculated from their SEM images.

ATR-FTIR Spectroscopy

Chemical analysis of electrospun PLGA, nano-HA and PLGA/nano-HA nanofibrous scaffolds was performed by ATR-FTIR spectroscopy. ATR-FTIR spectra of scaffolds were obtained on an Equinox 55 spectrometer (Bruker optics, Germany).

Experimental Design

Among various designs of experiment methods, the Central composite design (CCD) is more advantageous because this design takes into account interactions between parameters with less experiments. CCD was employed to study the effects of electrospinning parameters on the MFD of nanofibrous mats. The independent variables X_1 , X_2 , X_3 , X_4 , X_5 were as follows (low/high value): distance (cm) 5/35; nano-HA concentration ((w/w)%) 0/30; voltage (kV) 9/21, temperature ($^{\circ}$ C) 25/45 and flow rate (ml/h) 0.2/1.4, respectively. The ranges of the variables were selected from trial experiments and represented the attainable limits for nanofiber formation and/or equipment operation. The electrospinning parameters were coded at five levels as shown in *Table I*. Thirty two experiments, including fifteen factorial points and eleven axial points as well as six replicates at the center point were designed using CCD methodology. Six replications at the center of the design were used to estimate the pure error. The design matrix and results of the recorded mean diameter for every set of experiments are shown in *Table II*. Design of experiments (DOE) and features of Design Expert-7 Software (trial version, Stat-Ease Inc., USA) were utilized as well to determine the coefficients of mathematical modeling based on the response surface regression model. This software also produces analysis of variance (ANOVA) table to test lack of fit of the RSM-based models, and offers the graphic option to obtain a response surface plot for the selected parametric ranges of the developed response.

Variable	Low axial	Low factorial	Center	High factorial	High axial
	(-2)	(-1)	0	(+1)	(+2)
X ₁ (A)	5	10	15	20	25
X ₂ (B)	0	7.5	15	22.5	30
X ₃ (C)	9	12	15	18	21
X ₄ (D)	25	30	35	40	45
X ₅ (E)	0.2	0.5	0.8	1.1	1.4

X₁ (A) = Distance (cm)

X₂ (B) = Nano-HA concentration (w/w) %

X₃ (C) = Voltage (kV)

X₄ (D) = Temperature (°C)

X₅ (E) = Flow rate (ml/h)

TABLE II. Experimental conditions and their responses.

Run No.	X ₁ (A)	X ₂ (B)	X ₃ (C)	X ₄ (D)	X ₅ (E)	MFD (nm)
1	1	-1	-1	-1	-1	277
2	0	0	2	0	0	399
3	0	0	0	0	0	276
4	0	0	0	0	-2	237
5	1	1	-1	-1	1	288
6	0	0	0	0	0	277
7	2	0	0	0	0	379
8	0	0	0	-2	0	149
9	-2	0	0	0	0	115
10	1	1	1	-1	-1	318
11	1	1	1	1	1	415
12	0	0	-2	0	0	481
13	1	-1	1	1	-1	390
14	-1	-1	1	-1	-1	179
15	-1	1	-1	1	1	238
16	-1	-1	-1	-1	1	152
17	-1	1	-1	-1	-1	123
18	0	0	0	0	0	272
19	0	2	0	0	0	227
20	0	0	0	2	0	326
21	-1	-1	-1	1	-1	221
22	0	0	0	0	2	389
23	-1	1	1	-1	1	196
24	0	0	0	0	0	278
25	0	0	0	0	0	280
26	0	0	0	0	0	274
27	0	-2	0	0	0	233
28	-1	1	1	1	-1	252
29	1	-1	-1	1	1	376
30	-1	-1	1	1	1	290
31	1	1	-1	1	-1	352
32	1	-1	1	-1	1	332

RESULTS AND DISCUSSION

Fourier Transform Infrared Spectroscopy Study

The FTIR spectra of neat PLGA and PLGA/HA are shown in *Figure 1*. The scans showed an ester carbonyl stretch from the PLGA (C=O) at 1747 cm⁻¹ in all the scaffolds with no significant shift due to nano-HA interaction. Other major peaks observed were the C-O-C ether group at 1083 cm⁻¹, C-O stretch at 1128 cm⁻¹, A-type C-O-C symmetric stretching at 1181 cm⁻¹, O-H deformation at 1264 cm⁻¹, methyl group C-H stretching at 1452 cm⁻¹ and other methylene, methyl groups at 2800–3300 cm⁻¹. For the nanocomposite scaffolds, a PO₄³⁻ stretching (1030 cm⁻¹) and bending (570 cm⁻¹), typical of HA, were observed with intensities varying proportionally with the Nano-HA concentration.

Response Surface Methodology

The experimental process conditions and their responses are presented in *Table II*. A quadratic model for the average variations of PLGA/nHA nanofibers was chosen and fitted to the results. Eq. (1), found to be adequate for the MFD prediction of PLGA/nHA electrospun nanofibers.

$$MFD = 280.01 + 68.87 A + 46.62 D + 19.96 E - 15.39 B^2 + 37.11 C^2 \quad (1)$$

A, B, C, D and E are the coded values for distance, nano-HA concentration, applied voltage, temperature and flow rate, respectively.

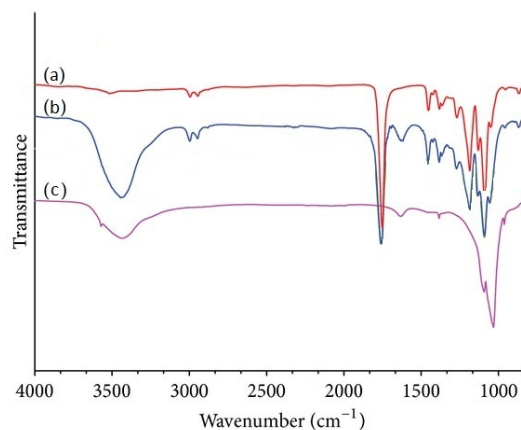


FIGURE 1. FTIR spectra of (a) PLGA nanofibers (b) PLGA-nanoHA nanofibers and (c) nano-HA.

Table III shows the results of ANOVA of the developed model. The regression equation obtained from the ANOVA showed that the R^2 was 0.938. However, since the model equations in our case include additional terms because of the five level independent variables, the adjusted R^2 (adj- R^2) for the degrees of freedom was chosen to be examined as well. Adj- R^2 is much less sensitive to the degrees of freedom and cannot be affected as seriously by including more terms in the model, while it is always lower than R^2 . Therefore, it is a better criterion of the goodness of the fit. The adj- R^2 value for the response was found to be equal to 0.985. It implies that the fitted model is significant in 95% confidence level (p -value < 0.05). The high value of R^2 indicates that the polynomial equation is capable of representing the system under the given experimental domain. Figures 2 and 3 represent predicted against actual values and residuals vs. predicted values for size, respectively.

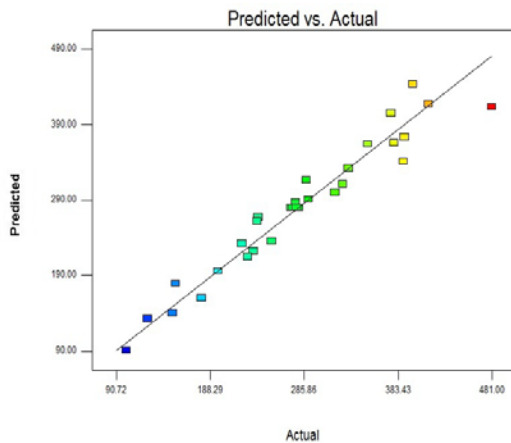


FIGURE 2. Predicted vs. actual values of nanofiber size.

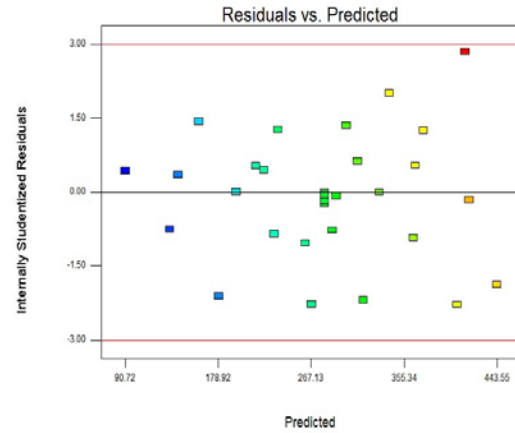


FIGURE 3. Residuals vs. predicted values of nanofiber size.

TABLE III. The ANOVA analysis using coded values.

Source	Sum of square	DOF	Mean square	P>F
Model	2.33E+05	20	11627.05	0.0016
Dist.	1.14E+05	1	1.14E+05	0.0003
Temp.	43605.38	1	43605.38	0.0013
Flow.	9560.04	1	9560.04	0.0098
Conc. ²	6944.38	1	6944.38	0.0241
Vol. ²	40404.38	1	40404.38	
Pure Error	40.83	5	8.17	
Total	2.48E+05	31		

Significant at 5% level ($P < 0.05$)

Effects of Parameters on MFD

Spinning Distance

The effect of spinning distance on MFD is illustrated in Figure 4(c). As shown, fiber diameter increased with increasing spinning distance. Increasing the spinning distance means that the electric field strength ($E=V/d$) will decrease, resulting in less acceleration, which leads to fibers with larger diameters. Spinning distance has two different effects on MFD. Longer spinning distance will provide more time not only to stretch the jet in the electric field but also to evaporate the solvent, thereby encouraging formation of thinner fibers. The balance between these two effects will determine the final fiber diameter.

Nano-HA Concentration

The effect of concentration on MFD is shown in Figure 4(a). It shows that there is a concave dependence curve between fiber diameter and concentration. As shown MFD decreased initially by increasing concentration and then increased. Increasing the nHA content initially decreased the fiber diameter probably due to the increase in conductivity of the solution and the surface charge density of the solution jet. But at higher concentrations, the diameter increased. This is probably due to the nHA agglomeration which prevents the formation of continuous fibers and also results in thicker fiber production. At higher concentrations, however, there are extensive chain entanglements, resulting in higher viscoelastic forces which tend to resist against the electrostatic stretching force.

Applied voltage

Figure 4(a) and Figure 4(b) show the effect of voltage on the mean fiber diameter. As shown, increasing the voltage resulted in an increase followed by a decrease in MFD. Applied voltage has two major different effects on fiber diameter. Firstly, increasing the applied voltage will increase the electric field strength and larger electrostatic stretching force causes the jet to accelerate more in the electric field, thereby favoring thinner fiber formation. On the other hand, the flight time of jet stream in the electrostatic field decreased with increasing applied voltage and the jet stream reached the collector before it could split into thinner streams. Also, there was not enough time for the evaporation of solvent. Thus, thicker fibers were collected on the collector. The combination of these two effects will determine the final fiber diameter. Hence, increasing applied voltage may decrease [22,23], increase [24,25] or may not change [21,26,27] the fiber diameter.

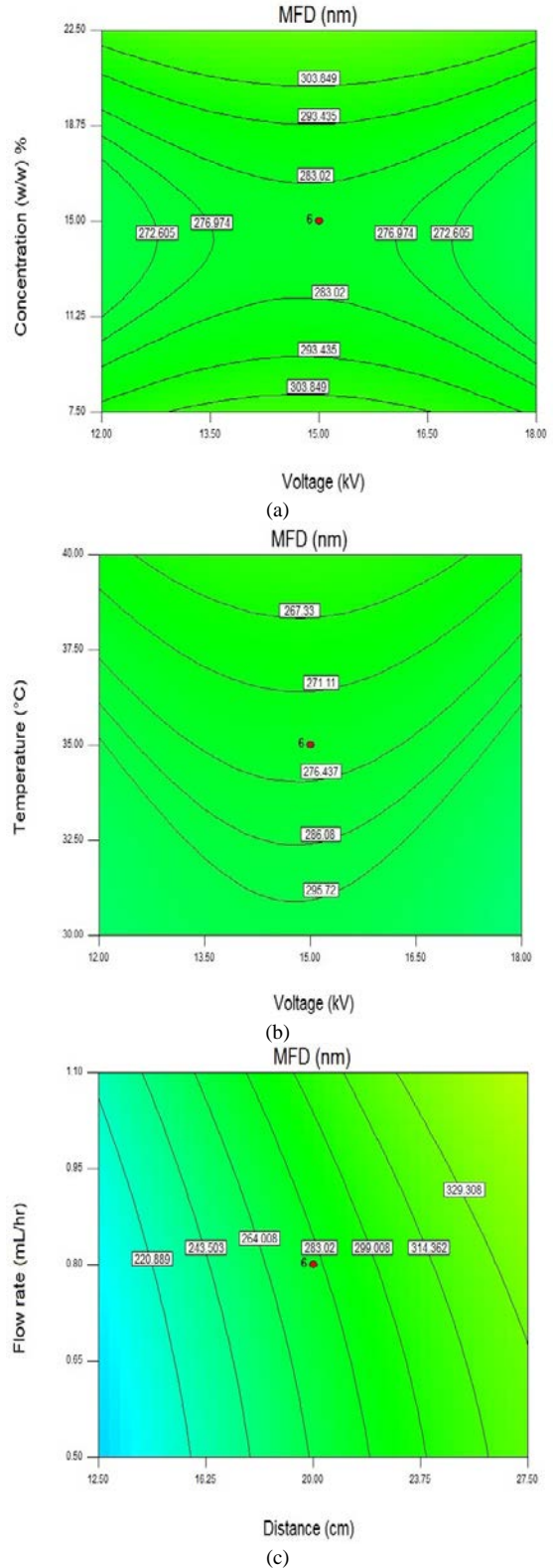


FIGURE 4. Contour plots of variables: (a) concentration vs. voltage (b) temperature vs. voltage (c) distance vs. flow rate.

Flow Rate

Flow rate of the polymer solution within the syringe is another important process parameter. It could affect the morphology of electrospun nanofibers such as fiber diameter. As shown in *Figure 4(c)*, MFD increased with increasing the flow rate of solution, which agrees with the previous studies [28,29]. Increasing the flow rate, more amount of solution is delivered to the tip of the needle enabling the jet to carry the solution away faster. This could bring about an increase in the jet diameter, favoring thicker fiber formation.

Temperature

Among the electrospinning parameters such as concentration, applied voltage, spinning distance and feeding rate, the temperature of the spinning process is another significant factor that influences the MFD of electrospun fibers as it could change the elastic properties of the polymer solution. *Figure 4(b)*, show the effect of temperature on the mean fiber diameter. As can be seen, for all concentrations, fiber diameter decreased by increasing the temperature. Mituppatham et al. [30] had proven that increasing temperature favors the thinner fiber diameter with polyamide-6 fibers for the inverse relationship between the solution viscosity and temperature. In consequence, the temperature facilitates the electrical stretching of the whipping jet by providing an adequately elastic response of the solution. Also, more solvent evaporated with increasing temperature, which resulted in thinner fiber formation.

Optimizing the Nanofiber Diameter

In this study, our goal is to minimize the average of nanofibers diameter. Optimization finds a good set of conditions that will meet the minimum diameter. The conditions for finest diameter estimated by the RSM equation were spinning distance (X_1) = 12.5 cm, nano-HA concentration (X_2) = 22.5 (w/w) %, applied voltage (X_3) = 14.7 kV, temperature (X_4) = 30 °C and flow rate (X_5) = 0.5 mL/h. The theoretical average fiber diameter under the above conditions was 107 nm. In order to investigate the reliability of the fibers produced from the electrospinning process, two tests were conducted to measure the fiber diameter from the given set of process parameters. The average nanofiber diameter was estimated to be 102 nm. SEM images of fibers at optimum conditions are shown in *Figure 5*. Comparing the experimental result with the predicted value under the same electrospinning settings shows that they are close to each other.

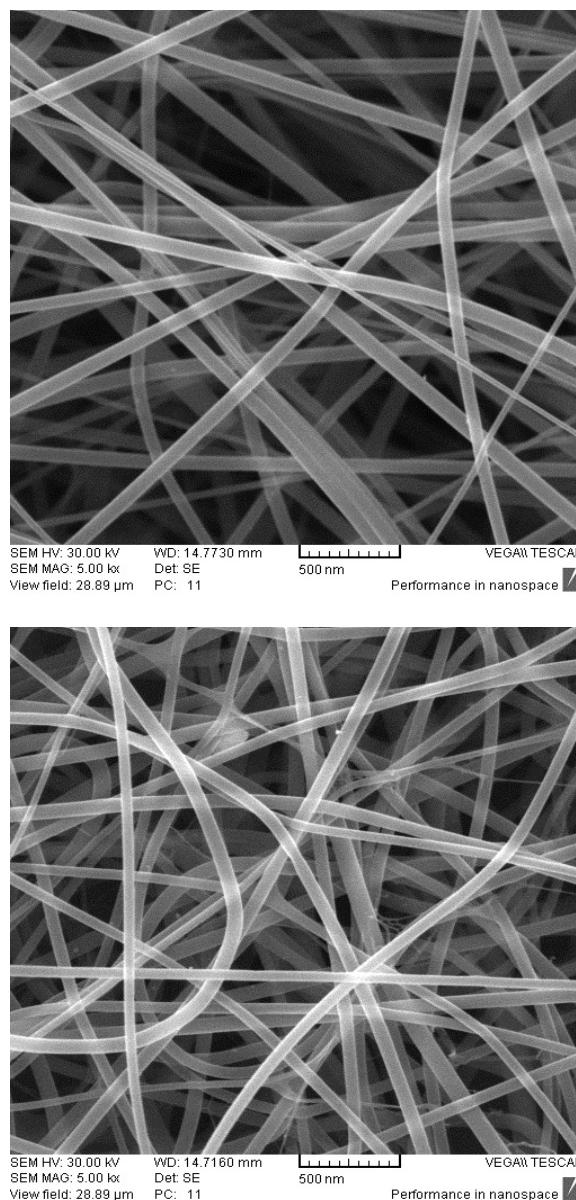


FIGURE 5. SEM images of nanofibers at optimum conditions.

CONCLUSION

In this study, nanofibrous nanocomposite scaffolds of nano-HA and PLGA were prepared using electrospinning method. The simultaneous effects of four processing variables, including nano-HA concentration, applied voltage, spinning distance, and flow rate on MFD, were investigated. Response surface methodology was used for modeling and optimizing of the average nanofiber diameters. Nano-HA concentration, spinning distance, voltage, temperature and flow rate were the studied factors for

this purpose. A quadratic equation for average fiber diameter was developed. Accuracy of the model was proved by comparing the estimated nanofiber diameter with the observed responses. The small differences of experimental data with predicted values, indicating the good prediction ability of the model. Prepared nano-HA/PLGA nanofibers are good candidates as local implantable scaffolds for bone tissue engineering.

REFERENCES

- [1] Ma Z, Kotaki M, Inai R, Ramakrishna S, "Potential of nanofiber matrix as tissue engineering scaffolds", *Tissue Eng*, 11(1), 2005, pp.101–109.
- [2] Ramakrishna S, Tan S-H, Inai R, et al, "Systematic parameter study for ultra-fine fiber fabrication via electro spinning process", *Polymer*, 46(16), 2005, pp. 6128-6134.
- [3] Thomas V, Jose M, Chowdhury S, et al, "Mechanomorphological studies of aligned nanofibrous scaffolds of polycaprolactone fabricated by electrospinning", *J Biomater Sci Poly Ed*, 17(9), 2006, pp. 969-984.
- [4] Sundaray B, Subramanian V, Natarajan TS, "Electrospinning of continuous aligned polymer fibers", *Appl Phys Lett*, 84(7), 2004, pp.1222.
- [5] Altman GH, Diaz F, Jakuba C, et al, "Silk-based biomaterials", *Biomaterials*, 24, 2003, pp. 401–416.
- [6] Doustgani A, Vasheghani-Farahani E, Soleimani M, " Aligned and random nanofibrous nanocomposite scaffolds for bone tissue engineering", *Nanomed J*, 1(1), 2013, pp. 20-27.
- [7] Nakhaei O and Shahtahmassebi N, " Study structural and up-conversion luminescence properties of polyvinyl alcohol/CaF₂:erbium nanofibers for potential medical applications", *Nanomed J*, 2(2), 2015, pp. 160-166.
- [8] Akhgari A and Rotubati MH, "Preparation and evaluation of electrospun nanofibers containing pectin and time-dependent polymers aimed for colonic drug delivery of celecoxib", *Nanomed J*, 3(1), 2016, pp. 43-48.
- [9] Doustgani A, Vasheghani-Farahani E, Soleimani M, et al, "Preparation and Characterization of Aligned and Random Nanofibrous Nanocomposite Scaffolds of Poly (VinylAlcohol), Poly (ϵ -Caprolactone) and Nanohydroxyapatite", *Int J Nanosci Nanotech*, 7(3), 2011, pp. 127-132.
- [10] Ghaee A, Shariaty-Niassar M, Barzin J, et al, "Chitosan/Polyethersulfone Composite Nanofiltration Membrane for Industrial Wastewater Treatment" , *Int J Nanosci Nanotech*, 9(4), 2013, pp. 213-220.
- [11] Doustgani A and Pedram MS, "Preparation and investigation of polylactic acid, calcium carbonate and polyvinylalcohol nanofibrous scaffolds for osteogenic differentiation of mesenchymal stem cells", *Nanomed J*, 3(2), 2016, pp. 109-114.
- [12] Gheisari H and Karamian E, " Preparation and characterization of hydroxyapatite reinforced with hardystonite as a novel bio-nanocomposite for tissue engineering", *Nanomed J*, 2(2), 2015, pp. 141-152.
- [13] Mirzaei E, Faridi-Majidi R, Shokrgozar MA, et al, "Genipin cross-linked electrospun chitosan-based nanofibrous mat as tissue engineering scaffold", *Nanomed J*, 1(3), 2014, pp. 137-146.
- [14] Naderizadeh B, Moghimi A, Shahi M, "Electrospun Nitrocellulose and Composite Nanofibers", *J nanostructures*, 2(3), 2012, pp. 287-293.
- [15] Doshi J and Reneker DH. "Electrospinning process and application of electrospun fibers", *Journal of Electrostatics*, 35(2), 1995, pp.1698–1703 .
- [16] Subbiah T, Bhat GS, Tock RW, et al, "Electrospinning of nanofibers", *J Appl Polym Sci*, 96, 2005, pp.557–569.
- [17] I. K. Kwon, S. Kidoaki, et al, "Electrospun nano- to microfiber fabrics made of biodegradable copolyesters: structural characteristics, mechanical properties and cell adhesion potential", *Biomaterials*, 26, 2004, pp. 3929-3939.
- [18] Heikkilä P and Harlin A, "Parameter study of electrospinning of polyamide-6", *Eur Polym J*, 44, 2008, pp. 3067–3079.
- [19] Gu SY, Ren J and Vancso GJ, "Process optimization and empirical modeling for electrospun polyacrylonitrile (PAN) nanofiber precursor of carbon nanofibers", *Eur Polym J*, 41, 2005, pp. 2559-2568.

- [20] Sukigara S, Gandhi M, Ayutsede J, et al, "Regeneration of *Bombyx mori* silk by electrospinning. Part 2: Process optimization and empirical modeling using response surface methodology", *Polymer*, 45, 2004, pp. 3701–3708.
- [21] Wang T and Kumar S, "Electrospinning of polyacrylonitrile nanofibers", *J Appl Polym Sci*, 102, 2006, pp. 1023–1029.
- [22] C. J. Buchko, L. C. Chen, Y. Shen, et al, "Processing and microstructural characterization of porous biocompatible protein polymer thin films", *Polymer*, 40, 1999, pp. 7397-7407.
- [23] Lee JS, Choi KH, Ghim HD, et al, "Role of molecular weight of atactic poly(vinyl alcohol) (PVA) in the structure and properties of PVA nanofabric prepared by electrospinning", *J Appl Polym Sci*, 93, 2004, pp.1638-1646.
- [24] Zhang C, Yuan X, Wu L, et al, "Study on morphology of electrospun poly(vinyl alcohol) mats", *Eur Polym J*, 41, 2005, pp. 423–432.
- [25] Li Q, Jia Z, Yang Y, Wang L, et al, "Preparation and properties of poly(vinyl alcohol) nanofibers by electrospinning", *Proceedings of IEEE International Conference on Solid Dielectrics*, Winchester, U.K. (2007).
- [26] Tan SH, Inai R, Kotaki M, et al, "Systematic parameter study for ultra-fine fiber fabrication via electrospinning process", *Polymer*, 46, 2005, pp. 6128–6134.
- [27] Sukigara S, Gandhi M, Ayutsede J, et al, "Regeneration of *Bombyx mori* silk by electrospinning—part 1: processing parameters and geometric properties". *Polymer*, 44, 2003, pp. 5721-5727.
- [28] Zong X, Kim K, Fang D, et al, "Structure and process relationship of electrospun bioabsorbable nanofibre membranes", *Polymer*, 43, 2002, pp. 4403–4412.
- [29] Li D and Xia Y, "Fabrication of Titania Nanofibers by Electrospinning", *Nano Lett*, 3, 2003, pp. 555–560.
- [30] Mit-uppatham C, Nithitanakul M and Supaphol P, "Ultrafine electrospun polyamide-6 fibers: Effect of solution conditions on morphology and average fiber diameter", *Macromol Chem Phys*, 205(17), 2004, pp. 2327–2338.

AUTHORS' ADDRESSES

Amir Doustgani

Ebrahim Ahmadi

University of Zanjan

Chemical Engineering Department

Zanjan, Zanajn 45156

IRAN, ISLAMIC REPUBLIC OF